Adaptive acoustooptic filter

Demetri Psaltis and John Hong

A new adaptive filter utilizing acoustooptic devices in a space integrating architecture is described. Two configurations are presented; one of them, suitable for signal estimation, is shown to approximate the Wiener filter, while the other, suitable for detection, is shown to approximate the matched filter.

I. Introduction

The design of optimum systems, in the classical sense, requires *a priori* some knowledge of the signals to be encountered. As a result, such systems perform poorly when the appropriate characteristics of the input signals are not known *a priori* sufficiently well or are time-varying. An adaptive processor has the ability to self-optimize by continually monitoring its performance and updating its parameters. Adaptive techniques have been applied to both spatial and temporal filtering domains. Specifically, adaptive techniques have been applied to antenna array processing by Appelbaum,[1] Widrow,[2] and others.[3,4] Applications to time domain problems include Lucky's work on data redundancy removal,[5] Sondhi's adaptive echo canceler,[6] Widrow's work on adaptive noise suppression,[7] Morgan and Craig's adaptive linear predictor,[8] and more.[9–11]

In the work on time domain problems cited above the adaptive filtering scheme is based on the orthogonality principle.[12] The basic idea behind the scheme is to control a variable filter so as to minimize the correlation between the input signal and the residual signal, which is the difference between the input signal and the filter output. A particular implementation of this scheme uses the transversal filter architecture, which consists of a tapped delay line, variable filter weights, and a summer that produces a weighted sum of delayed versions of the input signal as its output.

The linearity and parallel nature of the transversal filter arrangement, commonly called the correlation cancellation loop (CCL) system, make the optical implementation possible. The advantages of optical processors in terms of bandwidth and the large effective number of taps make such an implementation attractive. For example, acoustooptic devices (AODs), which can serve as optically tapped delay lines, are superior in terms of bandwidth to CCD implemented delay lines that are currently used in analog adaptive filters.[13,14] Several adaptive optical filter implementations have been previously proposed. Psaltis *et al.*[15,16] proposed use of an iterative electrooptic processor for adaptive spatial filtering of phased array antenna signals. Rhodes[17] described a system using acoustooptic and electrooptic modulators in a time integrating architecture to implement the CCL algorithm in the time domain, and VanderLugt[18] described an optical processor which is a frequency domain implementation of the CCL algorithm. Lee *et al.*[19] have devised an adaptive filter which suppresses narrowband interference from wideband signals using an acoustooptic spectrum analyzer with an array of electrooptic modulators in the spatial frequency plane which can adaptively excise strong narrowband components of the signal spectrum.

In this paper, we describe a new method for adaptive inverse filtering in the time domain. Two implementations are presented; the first, the passive processor, performs the inverse filtering operation, while the other, the active processor, is capable of performing adaptive matched filtering operations. Both processors are space integrating systems and do not require optically addressed, time integrating spatial light modulators. These architectures implement the CCL algorithm in the time domain and are structurally simpler than their frequency domain implemented counterparts. The implementations are strictly one dimensional, and thus it is possible to extend this concept to 2-D processing problems through the use of multichannel AODs.

The adaptive processors are discussed at the system level in Sec. II, and the optical implementations of the system blocks are described in Sec. III. The two optical configurations of the adaptive filters are described in Sec. IV.

II. Adaptive Estimation and Detection

The extraction of information from a signal corrupted by additive noise requires *a priori* knowledge of the properties of the desired signal and the noise. If the necessary information is known, the optimum linear filters can be designed to satisfy the specified performance criteria. The Wiener filter provides the minimum mean square error estimate of a signal in the

The authors are with California Institue of Technology, Department of Electrical Engineering, Pasadena, California 91125

Received 27 April 1984.
0003-6935/84/193475-07$02.00/0.

presence of additive noise, but it requires that the autocorrelations as well as the cross-correlation of the signal and the noise be known in advance. The filter that maximizes the output SNR is the matched filter which requires prior knowledge of the autocorrelation of the noise and also the desired signal waveform.

When the necessary correlation functions are not known *a priori*, they must be estimated adaptively from the past history of the signal and the limited and qualitative information that is available. We assume that the available information is as follows: the signal and noise are uncorrelated, and the signal is broadband, as in spread spectrum systems. We model the wideband signal as bandlimited white noise, so that $S_s(\omega)$, the spectral density of the wideband signal $s(t)$, is equal to $S_0 \operatorname{rect}[(\omega - \omega_0)/\Delta\omega]$, where ω_0 is the center frequency of the signal and $\Delta\omega$ is its bandwidth. The spectral density of the interference $n(t)$ is assumed to be unknown, and it is adaptively estimated.

Shown in Fig. 1 is a system diagram of the passive processor, which will be shown to adaptively perform an operation that approximates the Wiener filter under the conditions stated in the above paragraph. The two necessary operations in implementation of this filter are a convolution and a correlation. The convolver serves as the variable filter that is controlled by the correlator which estimates the correlation of the interference. The operation of the convolver and correlator blocks are described by the following input–output relations:

$$u(t) = \int_{-\infty}^{\infty} i_1(t-\tau) i_2(\tau) d\tau, \tag{1}$$

$$w(t) = \int_{-\infty}^{\infty} i_1(t+\tau) i_2^*(\tau) d\tau, \tag{2}$$

where $i_1(t)$ and $i_2(t)$ are the inputs to the blocks. Using Eqs. (1) and (2), we find the relationship between the input and output signals, $x(t)$ and $z(t)$, respectively, of the passive processor of Fig. 1:

$$\begin{aligned} z(t) &= x(t) - G \iint_{-\infty}^{\infty} z(\tau) x^*(\alpha-\sigma) x(t+\alpha-\tau-\sigma) d\alpha d\tau \\ &= x(t) - G \iint_{-\infty}^{\infty} z(\tau)[s^*(\alpha-\sigma) + n^*(\alpha-\sigma)] \\ &\quad \times [s(t+\alpha-\tau-\sigma) + n(t+\alpha-\tau-\sigma)] d\alpha d\tau, \end{aligned} \tag{3}$$

where σ is a time delay. Low input SNR, along with the assumption of the uncorrelatedness between the signal $s(t)$ and the noise $n(t)$, results in the reduction of Eq. (3) into

$$z(t) \cong x(t) - G \iint_{-\infty}^{\infty} z(\tau) n^*(\alpha-\sigma) n(t+\alpha-\tau-\sigma) d\alpha d\tau. \tag{4}$$

Fourier transformation of the above equation yields the approximate steady-state description:

$$Z(\omega) \cong X(\omega) - GZ(\omega)|N(\omega)|^2, \tag{5}$$

where $Z(\omega)$ and $X(\omega)$ are the Fourier transforms of $z(t)$ and $x(t)$, respectively, and $|N(\omega)|^2$ is the power spectrum of a sample realization of $n(t)$. Solving for $Z(\omega)$ gives

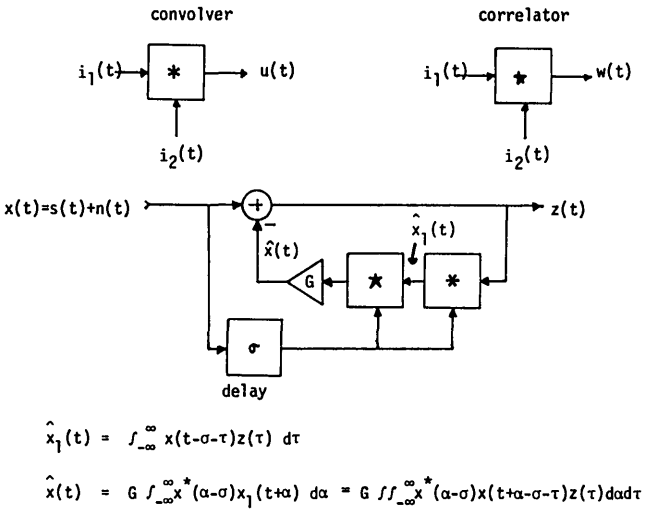

Fig. 1. Passive processor.

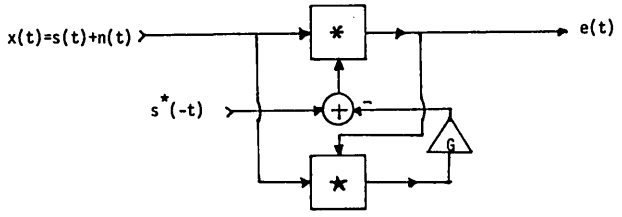

Fig. 2. Active processor.

$$Z(\omega) \cong \frac{X(\omega)}{1 + G|N(\omega)|^2} = \frac{1/G}{1/G + |N(\omega)|^2} X(\omega). \tag{6}$$

The input signal to the convolver and the correlator in Fig. 1 is delayed by the same amount, and, therefore, the output of the convolver–correlator combination $\hat{x}(t)$ becomes independent of the delay. This is an important result since it assures that the feedback signal $\hat{x}(t)$ is inphase with the input signal, and hence the system will be stable. With $G = 1/S_0$ and identifying $|N(\omega)|^2$ as the estimate of $S_n(\omega)$, the spectral density of $n(t)$, Eq. (6), describes the output of a Wiener filter.[20]

We now show that the active processor, shown in Fig. 2, adaptively performs matched filtering. The exact input–output relationship is given by

$$\begin{aligned} e(t) &= \int_{-\infty}^{\infty} x(t-\tau) s^*(-\tau) d\tau \\ &\quad - G \iint_{-\infty}^{\infty} x(t-\tau) x^*(\alpha) e(\tau+\alpha) d\alpha d\tau, \end{aligned} \tag{7}$$

where $e(t)$ is the output signal of the active processor. The assumption of low input SNR along with the conditions stated previously allows the following approximate form of Eq. (7):

$$\begin{aligned} e(t) &\cong \int_{-\infty}^{\infty} x(t-\tau) s^*(-\tau) d\tau \\ &\quad - G \iint_{-\infty}^{\infty} n(t-\tau) n^*(\alpha) e(\tau+\alpha) d\alpha d\tau. \end{aligned} \tag{8}$$

The Fourier transform of the output signal $e(t)$ is readily found to be

$$E(\omega) \cong \frac{X(\omega)S^*(\omega)}{1 + G|N(\omega)|^2} \cong \frac{X(\omega)S^*(\omega)}{G|N(\omega)|^2}, \tag{9}$$

where $E(\omega)$ is the Fourier transform of $e(t)$, and the last result is valid if the feedback gain G is made sufficiently large. If the input SNR is high, it is evident from the equations that the system will equalize the spectrum of the total input signal while simultaneously performing a matched filtering operation. Identifying $|N(\omega)|^2$ as the power spectrum of the noise, Eq. (9) is the matched filter result.[20] Thus, from Eqs. (6) and (9), both active and passive processors share the common property of suppressing strong narrowband components that are present in the input signal. This property, commonly called line cancellation, is suitable in environments where sinusoidal jammers are present for either estimation or detection of broadband spread spectrum signals.

III. Optical Filters

The two adaptive filters that we described in the previous section are both implemented with a convolver and a correlator. There are several possible ways to implement an optical correlator/convolver. In selecting an implementation that is best suited for this application, we must consider the following requirements: (a) The optical filters should be capable of processing broadband signals (1-GHz bandwidth) to be applicable to spread spectrum systems. This requirement suggests an acoustooptic implementation. (b) The impulse response of the convolver and the correlator must be dynamically controllable. The impulse response of the correlator, in particular, is also a broadband signal. (c) The two filters must be compatible with one another; the impulse response of the convolver is determined by the output of the correlator, and the output of the convolver is one of the inputs to the correlator. (d) We must select architectures that have the maximum linear dynamic range possible. Adaptive filters are typically used to process signals with very low SNRs; this implies that they must have a sufficient dynamic range to place very deep nulls at the frequencies where the interference occurs in order to suppress it effectively. The acoustooptic space integrating convolver, consisting of two counterpropagating AODs, an integrating lens, and a single detector, is well suited for this application in that its two inputs and the output are broadband electrical signals, and a very high dynamic range is possible in this architecture. One potential difficulty with using this type of convolver is the fact that its output is time-compressed by a factor of 2, and thus it cannot be directly correlated with the input signal as required for adaptive filtering. A second problem is that correlation cannot be readily performed with this architecture; one of the input signals must be time reversed before it is applied to the convolver to compute the correlation with such a system. These two problems combine to provide a solution in this case. We will show that a space integrating correlator can be implemented with two copropagating AODs if one of the inputs to the correlator is time compressed. The output of the space integrating convolver can thus be used as one of the inputs to such a correlator. In this section we describe a specific coherent realization of the acoustooptic convolver and correlator blocks. Several variations of these processors are possible, including an incoherent implementation. We begin with the description of the convolver shown in Fig. 3. It consists of two AODs with copropagating acoustic signals. The 1:1 imaging system between the AODs provides the coordinate inversion of one signal with respect to the other which is necessary for the convolution. Let $s_1(t)$ and $s_2(t)$ which are of the form, $s(t) = a(t)\cos[\omega_0 t + p(t)] = \mathrm{Re}[\mathbf{a}(t)\exp(j\omega_0 t)]$, represent the signals applied to the AODs; the complex envelope, $\mathbf{a}(t) = a(t)\exp[jp(t)]$, is the modulating signal, and ω_0 is the center frequency of the AODs. The first AOD in Fig. 3 is illuminated by a collimated coherent light beam incident at the Bragg angle θ_B (Ref. 21):

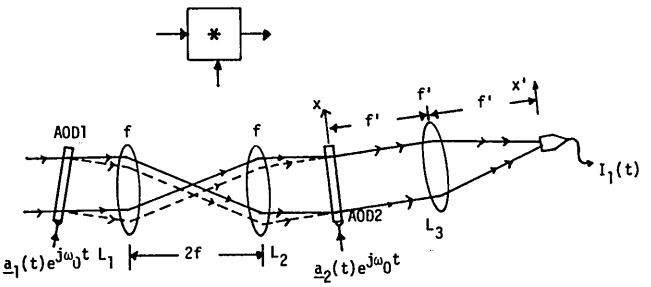

Fig. 3. Space integrating optical convolver.

$$\sin\theta_B = \lambda\omega_0/4\pi v, \tag{10}$$

where λ is the wavelength of light in the acoustooptic crystal, and v is the speed of sound in the crystal.

The interaction between the acoustic wave induced by the signal $s_1(t)$ and the optical field causes some of the incident light to be diffracted, and since the AODs are operated in the Bragg regime, only first-order diffraction is appreciable. For a more compact analysis, the induced acoustic signal in the AOD is treated as the system input; i.e., the fixed delay between the applied electrical signal and the acoustic signal is ignored. The final results, however, are strictly equivalent. In the actual implementation, additional delays will be necessary to compensate for the delays intrinsic to the acoustooptic system. For weak modulation, the optical field at the exit plane of AOD1 is given by[22]

$$\begin{aligned} A(x,t) &\propto \{\exp(-j2\pi\sin\theta_B x/\lambda) \\ &\quad + j(m/2)\mathbf{a}_1^*(t - x/v)\exp[-j\omega_0(t - x/v)] \\ &\quad \times \exp(-j2\pi\sin\theta_B x/\lambda)\}\,\mathrm{rect}(x/W) \\ &\propto [\exp(-j2\pi\sin\theta_B x/\lambda) + j(m/2)\mathbf{a}_1^*(t - x/v)\exp(-j\omega_0 t) \\ &\quad \times \exp(j2\pi\sin\theta_B x/\lambda)]\,\mathrm{rect}(x/W), \end{aligned} \tag{11}$$

where m is a constant, x is along the direction of the acoustic wave propagation, and W is the aperture size

of the AOD; note that the Bragg condition, Eq. (10), was used to derive the last line of Eq. (11). The first term on the right-hand side of Eq. (11) corresponds to the dc or undiffracted light which is unmodulated to first order. The second term corresponds to the (−1) diffracted order, which is modulated by $\mathbf{a}_1^*(t - x/v)$, Doppler shifted by $-\omega_0$, and deflected by an angle $2\theta_B$. The amplitude distribution, $A_1(x,t)$ in Eq. (11), is then imaged onto the second AOD by lenses $L1$ and $L2$; the imaging reverses the spatial coordinate x. The second AOD is positioned at the Bragg angle with respect to the dc component from AOD1, and, therefore, a portion of it is diffracted at an angle $2\theta_B$ by AOD2. The major portion of the diffracted beam from AOD1 passes through AOD2 undiffracted, since it is not Bragg-matched, and it propagates in the same direction as the beam diffracted by AOD2. The remaining components of the light at the exit of AOD2 are angularly separated from these two components and, therefore, can be blocked at the focal plane of lens $L3$. The two components of interest are given by

$$A_2(x,t) \propto [\mathbf{a}_2(t - x/v)\exp(-j2\pi \sin\theta_B x/\lambda)\exp(j\omega_0 t) + \mathbf{a}_1^*(t + x/v)\exp(-j2\pi \sin\theta_B x/\lambda) \times \exp(-j\omega_0 t)]\,\mathrm{rect}(x/W). \quad (12)$$

The first term on the right-hand side of Eq. (12) is the (+1) diffracted order from AOD2, which is modulated by $\mathbf{a}_2(t - x/v)$, Doppler shifted by ω_0, and deflected from the dc by $2\theta_B$; this beam is collinear with the (−1) diffracted beam from AOD1 [i.e., the second term in Eq. (12)]. The light amplitude at the back focal plane of lens $L3$ is the Fourier transform of Eq. (12). A detector with an active area sufficiently large to integrate the entire transform is placed at the Fourier plane, and the resulting photocurrent is

$$I_1(t) \propto \int_{-T/2}^{T/2} |\mathbf{a}_1(t+\tau)|^2 d\tau + \int_{-T/2}^{T/2} |\mathbf{a}_2(t-\tau)|^2 d\tau + 2\,\mathrm{Re}\left\{\exp(j2\omega_0 t)\int_{-T2}^{T/2} \mathbf{a}_1(t+\tau)\mathbf{a}_2(t-\tau)d\tau\right\}, \quad (13)$$

where $\tau = x/v$, and T is the acoustic delay through the aperture of the AOD, i.e., $T = W/v$. The first two terms on the right-hand side of Eq. (13) are low frequency components, and they are removed by filtering. The third term is the desired operation which is the convolution of $\mathbf{a}_1(t)$ and $\mathbf{a}_2(t)$. The convolution is compressed in time by a factor of 2 and translated to twice the original carrier freqeuncy. Notice that in both passive and active processors, the time compressed output of the convolver is one of the inputs to the correlator. Thus the correlator must be designed to accept a time compressed signal (by a factor of 2) in one of its input ports.

In contrast to convolution which requires an inversion of a coordinate, correlation requires that one of the input signals be in motion with respect to the other with no coordinate inversion. Referring to Fig. 4, the correlator consists of two identical AODs with counter-propagating acoustic signals; ω_0 and $2\omega_0$ are the carrier frequencies of the signals driving AOD3 and AOD4, respectively. The imaging system reverses the spatial

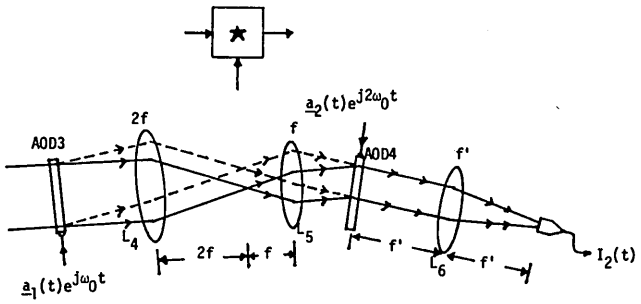

Fig. 4. Space integrating optical correlator.

coordinate of the signal in AOD3, so that the two signals are copropagating at AOD4. The imaging system has a 2:1 demagnification ratio, so that the velocity of the image of the light that is diffracted by AOD3 is half of that of the acoustic signal in AOD4. Thus the signals in the AODs continuously translate with respect to each other. The undiffracted beam from AOD3 is incident at the Bragg angle of AOD4 corresponding to its $2\omega_0$ center frequency. The demagnification by a factor of 2 increases the angular separation between the diffracted and undiffracted beams from AOD3 at the plane of AOD4. Therefore, the two diffracted beams from AOD3 and AOD4 are parallel to one another when they enter lens $L6$. $L6$ forms the Fourier transform of the light exiting AOD4, and a photodetector spatially integrates the entire spectrum. Through a development similar to that illustrated for the convolver, we find that the photocurrent from the detector in Fig. 4 is

$$I_2(t) \propto \int_{-\infty}^{\infty}\left|\int_{-T/4}^{T/4}[\mathbf{a}_1(t+2\tau)\exp(j\omega_0 t) + \mathbf{a}_2(t+\tau)\exp(j2\omega_0 t)]\exp(jk\tau)d\tau\right|^2 dk \propto \int_{-T/4}^{T/4}|\mathbf{a}_1(t+2\tau)|^2 d\tau + \int_{-T/4}^{T/4}|\mathbf{a}_2(t+\tau)|^2 d\tau + 2\,\mathrm{Re}\left\{\exp(j\omega_0 t)\int_{-T/4}^{T/4}\mathbf{a}_1^*(t+2\tau)\mathbf{a}_2(t+\tau)d\tau\right\}, \quad (14)$$

where k is the spatial frequency variable at the output plane. The limits of integration of the correlator are half of those of the convolver. This implies that the apertures of the AODs used in the correlator must be twice as long as those in the convolver to obtain equal integration limits. Unilluminated portions of the AODs in the correlator and the convolver can be used for introducing delays. The third term is the desired operation which resembles a correlation translated to the carrier frequency ω_0. If $\mathbf{a}_2(t) = \mathbf{a}_3(2t)$, the third term of Eq. (14) becomes

$$= 2\,\mathrm{Re}\left[\exp(j\omega_0 t)\int_{t-T/2}^{t+T/2}\mathbf{a}_1^*(\alpha)\mathbf{a}_3(t+\alpha)d\alpha\right], \quad (15)$$

which is a finite aperture correlation of the signals $\mathbf{a}_1(t)$ and $\mathbf{a}_3(t)$ placed on the carrier frequency ω_0.

IV. Adaptive Optical Processor Implementations

A schematic diagram of the optically implemented passive processor is shown in Fig. 5. Through use of a beam splitter, both the convolver and correlator have

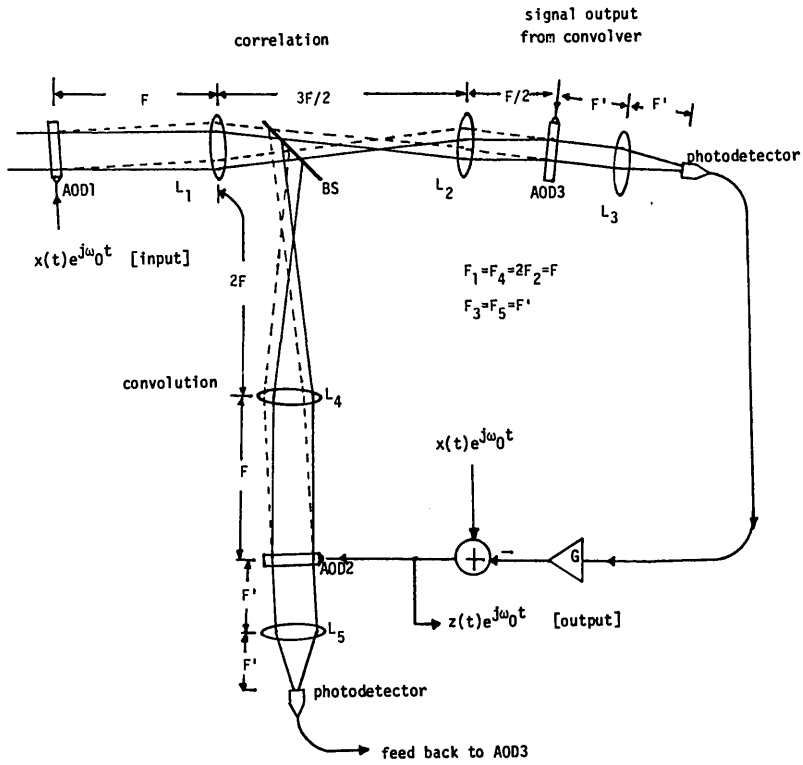

Fig. 5. Adaptive optical processor (passive).

been incorporated into one system requiring only one light source and three AODs. The correlator and convolver share, in effect, the AOD which is driven by the system input signal $x(t)$. The input signal, translated in frequency to ω_0, is applied to AOD1 and the summing node before entering AOD2. The convolution is performed by the lower leg of the processor and the correlation by the upper leg. As shown in the previous section, the optical convolver takes its two inputs, each at the carrier frequency ω_0 and gives their convolution, compressed in time by a factor of 2 and translated to $2\omega_0$, as its output. This output is then used to drive AOD3 of the correlator; recalling that to achieve a proper correlation, one of the correlator inputs must be time compressed by a factor of 2 and translated to $2\omega_0$, we see that its output is free of time scaling problems. This signal is then subtracted from the input signal to form the system output $z(t)$ which is fed back to the convolver via AOD2. The delay element which is necessary in the passive processor can be realized simply by translation of AOD1 along the direction in which the acoustic signal propagates.

We now derive the output of the optical passive processor that is obtained under the conditions stated in Sec. II. We begin by stating the mathematical operations performed by the optically implemented blocks of Figs. 1 and 2; with i_1 and i_2 as the inputs of the blocks, the convolver block output is given by

$$u(t) = (1/T)\int_{-T/4}^{T/4} i_1(t+\tau)i_2(t-\tau)d\tau, \tag{16}$$

and the correlator block output is given by

$$w(t) = (1/T)\int_{-T/4}^{T/4} i_1^*(t+2\tau)i_2(t+\tau)d\tau. \tag{17}$$

Equations (16) and (17) are simply Eqs. (13) and (14), respectively, with the carrier frequencies suppressed. These integals are different from their counterparts found in Eqs. (1) and (2) in two important ways. First, Eqs. (16) and (17) have finite limits of integration limited by the maximum transit delay time of the AODs. Also the arguments of the integrand are different, and these differences reflect the time compression problems of the optical convolver and correlator referred to earlier. In both cases, the integration limits extend from $-T/4$ to $T/4$, where T is the aperture of each AOD in units of time. With Eqs. (16) and (17), the input–output equation of the passive processor is

$$z(t) = x(t) - (G/T^2)\iint_{-T/4}^{T/4} x^*(t+2v-\sigma) \times x(t+\tau+v-\sigma)z(t-\tau+v)d\tau dv, \tag{18}$$

where, as in Sec. II, $z(t)$ is the system output, and $x(t) = s(t) + n(t)$ is the input; $s(t)$ is the broadband signal, and $n(t)$ is the narrowband interference. The delay element σ causes the broadband components to become decorrelated so that the narrowband components dominate the double integral of Eq. (18) yielding

$$z(t) = x(t) - (G/T^2)\iint_{-T/4}^{T/4} n^*(t+2v-\sigma) \times n(t+\tau+v-\sigma)z(t-\tau+v)d\tau dv. \tag{19}$$

Fourier transformation then yields

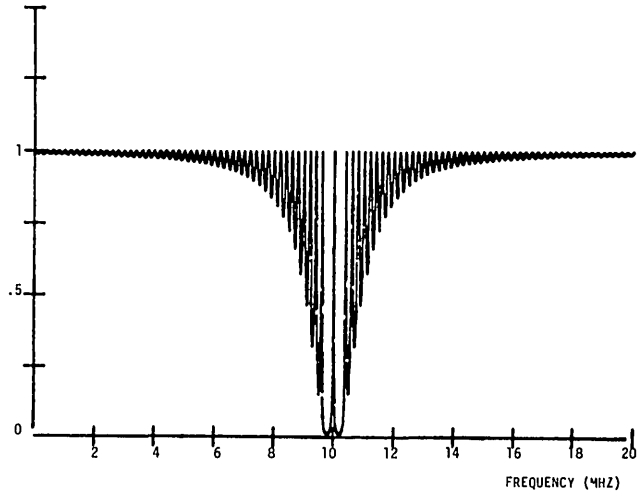

Fig. 6. Passive processor response to two jammers: $f_1 = 9.8$ MHz, $f_2 = 10.2$ MHz, $T = 10$ μsec.

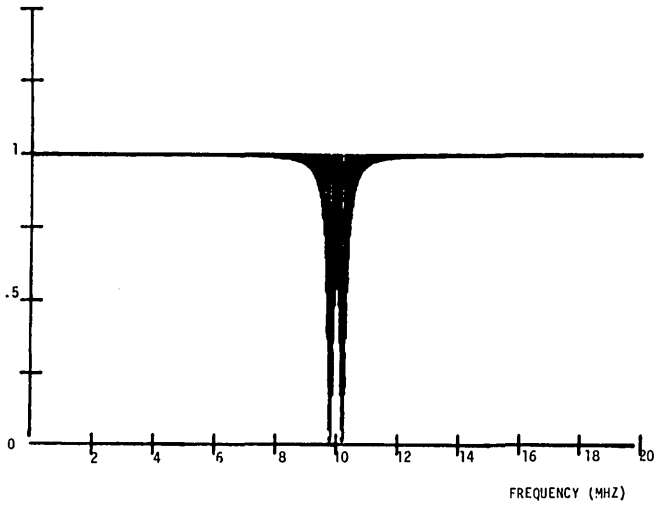

Fig. 7. Passive processor response to two jammers: $f_1 = 9.8$ MHz, $f_2 = 10.2$ MHz, $T = 50$ μsec.

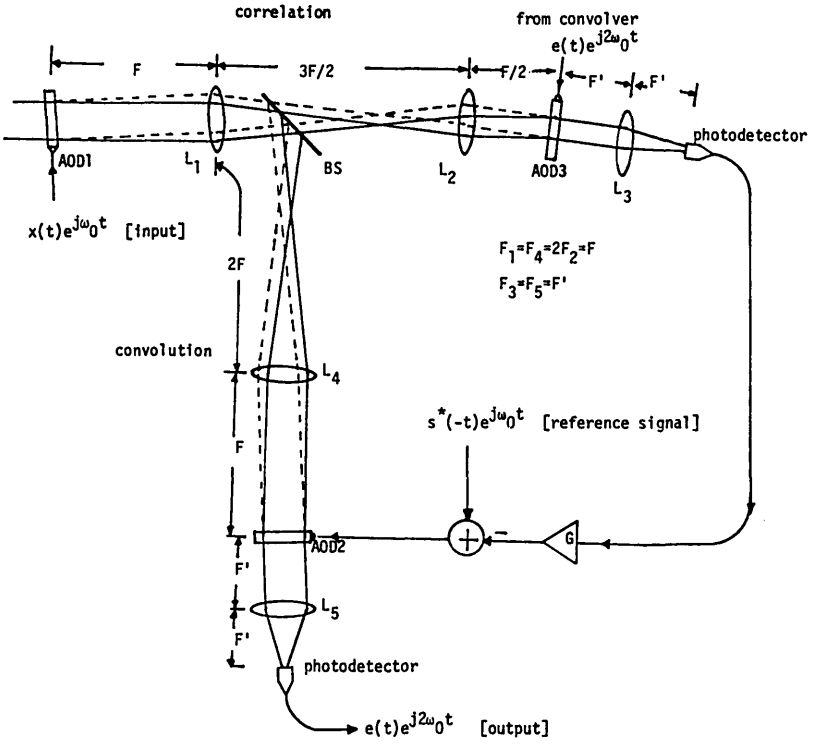

Fig. 8. Adaptive optical processor (active).

$$Z(\omega) \cong X(\omega) - (G/4\pi^2) \iint_{-\infty}^{\infty} N^*(\alpha) \times N(\beta) \exp[-j(\beta-\alpha)\sigma] Z(\omega+\alpha-\beta) \times \operatorname{sinc}[(\omega-\alpha)T/4\pi] \operatorname{sinc}[(\omega+\alpha-2\beta)T/4\pi] d\alpha d\beta. \quad (20)$$

The double integral of (20) can be approximated by a single integral since it becomes appreciably large only near the region $\alpha = \beta$, so that

$$Z(\omega) \cong X(\omega) - (G/4\pi^2) Z(\omega) \int_{-\infty}^{\infty} |N(\alpha)|^2 \times \operatorname{sinc}^2[(\omega-\alpha)T/4\pi] d\alpha. \quad (21)$$

Solving for $Z(\omega)$ gives

$$Z(\omega) \cong \frac{X(\omega)}{1 + (G/4\pi^2) \int_{-\infty}^{\infty} |N(\alpha)|^2 \operatorname{sinc}^2[(\omega-\alpha)T/4\pi] d\alpha}. \quad (22)$$

Except for the presence of the sinc function in the denominator due to the finite apertures of the AODs, Eq. (22) is quite similar to the Wiener result, Eq. (6). Shown on Figs. 6 and 7 are plots of $Z(\omega)/X(\omega)$ for an input consisting of two sinusoids, one at 9.8 MHz and the other at 10.2 MHz; the first plot is for $T = 10$ μsec, while the second is for $T = 50$ μsec. Clearly, the finite aperture of the AODs limit the resolving power of the

processor to distinguish between the various jamming signals present at the input.

The optically implemented active processor is shown schematically in Fig. 8; the active system differs from the passive only in its electrical interconnections. Here the output of the system is a time compressed signal since it is taken at the output of the convolver; this presents no problems since the output signal is a correlation peak, and we are interested in detection rather than estimation. As in the passive case, the convolver output drives AOD3 of the correlator. The correlator output is then subtracted from the time reversed reference signal (the matched filter impulse response) to form the input to AOD2 of the convolver; note that even though the output is time compressed, the time scaling is compatible for all the signals within the system. To see this more precisely, we examine the input–output equation for the active system; using Eqs. (16) and (17), we obtain

$$e(t) = (1/T)\int_{-T/4}^{T/4} x(t+\tau)s^*(\tau - t)d\tau - (G/T^2)\iint_{-T/4}^{T/4} x(t+\tau)x^*(t-\tau+2v)e(t-\tau+v)dvd\tau, \tag{23}$$

where $e(t)$ is the system output. Under low SNR conditions, Eq. (23) can be approximated by

$$e(t) \cong (1/T)\int_{-T/4}^{T/4} x(t+\tau)s^*(\tau - t)d\tau - (G/T^2)\iint_{-T/4}^{T/4} n(t+\tau)n^*(t-\tau+2v)e(t-\tau+v)dvd\tau, \tag{24}$$

The output spectrum is easily calculated from Eq. (24) to be

$$E(\omega) \cong \frac{(1/2\pi)\int_{-\infty}^{\infty} X(\alpha)S^*(\omega-\alpha)\,\mathrm{sinc}[(\omega-2\alpha)T/4\pi]a}{1+(G/4\pi^2)\int_{-\infty}^{\infty}|N(\alpha)|^2\,\mathrm{sinc}^2[(\omega-2\alpha)T/4\pi]d\alpha}. \tag{25}$$

Aside from the appearance of the sinc functions which arise due to the finite apertures of the AODs and the time compression, Eq. (25) is quite similar to Eq. (9), the matched filter result.

V. Conclusion

Two adaptive systems particularly suitable for use in narrowband jamming noise environments have been presented. The passive system has been shown to be appropriate for estimation purposes while the active, for signal detection. A particularly interesting extension of this work is the implementation of time–space adaptive filters for processing broadband signals from phased array antennas. The processors described in this paper are temporal filters, but since they are implemented in only one dimension, it is possible, through use of multiple transducer AODs, to implement a 2-D time–space adaptive filter. The 1-D processors are currently being built in the laboratory, and future research will include the experimental verification of the operation of the systems as well as statistical characterization of the effects of the finite apertures of the AODs and detector noise.

This work is supported by the Rome Air Development Center.

References

1. A. P. Appelbaum, "Adaptive Arrays," IEEE Trans. Antennas. Propag. **AP-24,** 585 (1976).
2. B. Widrow, P. E. Mantey, L. J. Griffiths, and B. B. Goode, "Adaptive Antenna Systems," Proc. IEEE **55,** 2143 (1976).
3. K. K. Scott, "Transversal Filter Techniques for Adaptive Array Applications," Proc. IEE **130,** Parts F+H, 29 (Feb. 1983).
4. R. Riegler and R. Compton, Jr., "An Adaptive Array for Interference Rejection," Proc. IEEE **61,** 748 (1973).
5. R. W. Lucky, "Adaptive Redundancy Removal in Data Transmission," Bell Syst. Tech. J. **47,** 549 (1968).
6. M. M. Sondhi, "An Adaptive Echo Canceller," Bell Syst. Tech. J. **46,** 497 (1967).
7. B. Widrow *et al.*, "Adaptive Noise Cancelling: Principles and Applications," Proc. IEEE **63,** 1692 (1975).
8. D. R. Morgan and S. E. Craig, "Real Time Adaptive Linear Prediction Using the Least Mean Square Gradient Algorithm," IEEE Trans. Acoust. Speech, Signal Process. **ASSP-24,** 494 (1976).
9. J. E. Bowers, G. S. Kino, D. Behar, and H. Olaisen, "Adaptive Deconvolution Using SAW Storage Correlators," IEEE Trans. Microwave Theory Tech. **MTT-29,** 491 (1981).
10. L. J. Griffiths, "Rapid Measurement of Instantaneous Frequency," IEEE Trans. Acoust. Speech, Signal Process. **ASSP-23,** 209 (1975).
11. J. Koford and G. Grover, "The Use of An Adaptive Threshold Element to Design a Linear Optimal Pattern Classifier," IEEE Trans. Inf. Theory **IT-12,** 42 (1966).
12. A. Papoulis, *Probability, Random Variables, Stochastic Processes* (McGraw-Hill, New York, 1965).
13. M. White, I. A. Mack, G. M. Borsuk, D. R. Lampe, and F. J. Kub, "CCD Adaptive Discrete Analog Signal Processing," IEEE J. Solid-State Circuits **SC-14,** 132 (1979).
14. C. F. N. Cowan, J. W. Arthur, J. Mavor, and P. B. Denyer, "CCD Based Adaptive Filters: Realization and Analysis," IEEE Trans. Acoust. Speech Signal Process **ASSP-29,** 220 (1981).
15. D. Psaltis *et al.*, "Iterative Color-Multiplexed Electrooptical Processor," Opt. Lett. **4,** 348 (1979).
16. D. Psaltis *et al.*, "Iterative Optical Processor for Adaptive Phase Array Radar Applications," Proc. Soc. Photo-Opt. Instrum. Eng. **180,** 114 (1979).
17. J. F. Rhodes, "Adaptive Filter with a Time-Domain Implementation Using Correlation Cancellation Loops," Appl. Opt. **22,** 282 (1983).
18. A. VanderLugt, "Adaptive Optical Processor," Appl. Opt. **21,** 4005 (1982).
19. J. N. Lee, N. J. Berg, and P. S. Brody, "High Speed Adaptive Filtering and Reconstruction of Broadband Signals Using Acoustooptic Techniques," in *Proceeding, Ultrasonics Symposium* (1980), pp. 488–491.
20. W. Davenport and W. Root, *Introduction to Theory of Random Signals and Noise* (McGraw-Hill, New York, 1967).
21. A. Yariv, *Quantum Electronics* (Wiley, New York, 1967).
22. W. T. Rhodes, "Acousto-Optic Signal Processing: Convolution and Correlation," Proc. IEEE **69,** 65 (1981).